iScience

CellPress

Article

Abnormal Behavior of Zebrafish Mutant in Dopamine Transporter Is Rescued by Clozapine

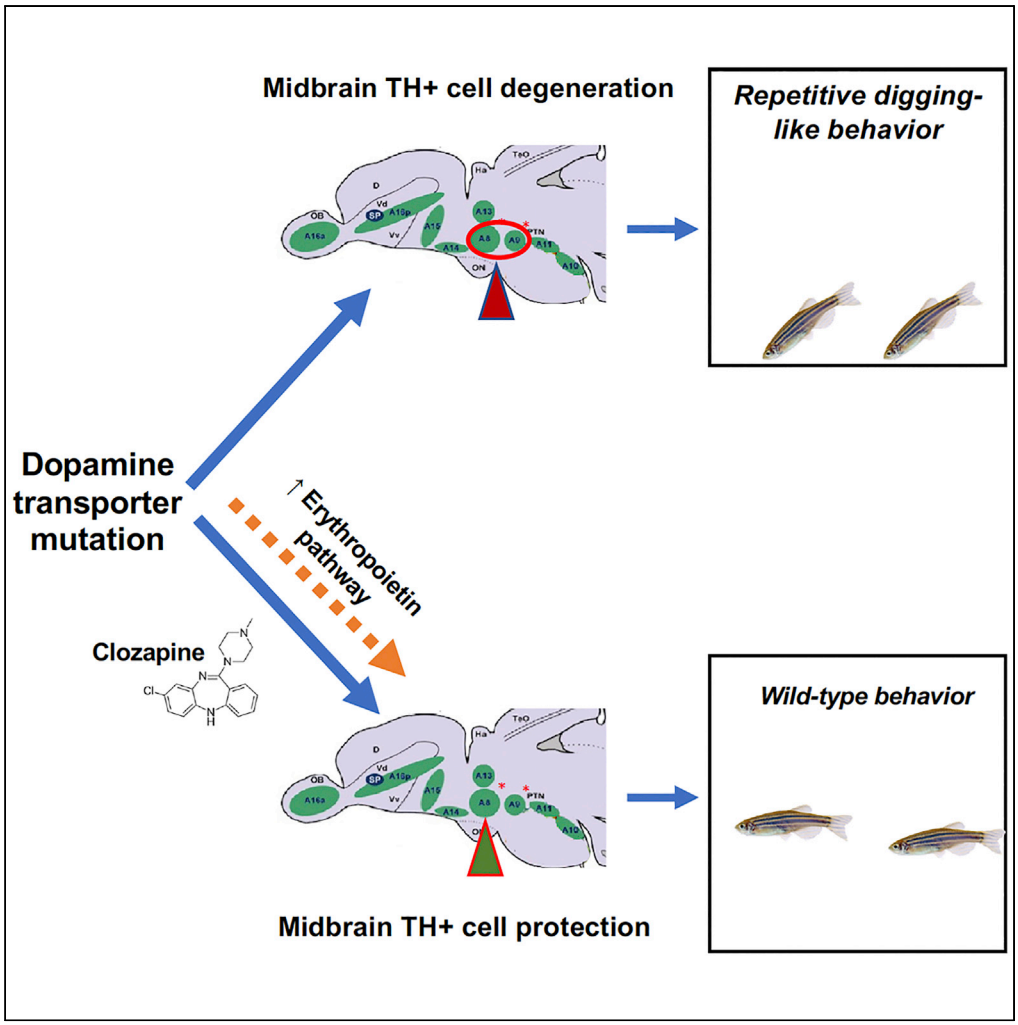

Guangliang Wang, Guoqiang Zhang, Zhuyun Li, ..., Peixin Zhu, David J. Glass, Mark C. Fishman

mark_fishman@harvard.edu

HIGHLIGHTS

DAT mutation in zebrafish causes digging behavior and loss of specific midbrain neurons

Clozapine restores normal behavior and neuronal morphology of mutant fish

Clozapine increases expression of erythropoietin pathway genes

Transgenic expression of erythropoietin partially rescues the mutant behavior

Wang et al., iScience 17, 325–333
July 26, 2019
https://doi.org/10.1016/j.isci.2019.06.039

iScience

CellPress

Article

Abnormal Behavior of Zebrafish Mutant in Dopamine Transporter Is Rescued by Clozapine

Guangliang Wang,[1] Guoqiang Zhang,[1] Zhuyun Li,[1] Caroline H. Fawcett,[1] Matthew Coble,[1] Maria X. Sosa,[1] Tingwei Tsai,[1] Kimberly Malesky,[1] Stefan J. Thibodeaux,[1] Peixin Zhu,[1] David J. Glass,[1] and Mark C. Fishman[2,3,*]

SUMMARY

Dopamine transporter (SLC6A3) deficiency causes infantile Parkinson disease, for which there is no effective therapy. We have explored the effects of genetically deleting SLC6A3 in zebrafish. Unlike the wild-type, *slc6a3*−/− fish hover near the tank bottom, with a repetitive digging-like behavior. *slc6a3*−/− fish manifest pruning and cellular loss of particular tyrosine hydroxylase-immunoreactive neurons in the midbrain. Clozapine, an effective therapeutic for treatment-resistant schizophrenia, rescues the abnormal behavior of *slc6a3*−/− fish. Clozapine also reverses the abnormalities in the A8 region of the mutant midbrain. By RNA sequencing analysis, clozapine increases the expression of erythropoietin pathway genes. Transgenic over-expression of erythropoietin in neurons of *slc6a3*−/− fish partially rescues the mutant behavior, suggesting a potential mechanistic basis for clozapine's efficacy.

INTRODUCTION

The dopamine transporter (DAT) is responsible for the reuptake of dopamine into presynaptic terminals and is responsible for the termination of dopamine's effect. Because altered dopamine signaling in the brain has been associated with a host of disorders, including Parkinson disease, schizophrenia, bipolar disease, and attention deficit disorder, DAT function has been the focus of genetic studies in several species. In humans, loss of function of DAT causes infantile Parkinson disease, with dystonia, rigidity, bradykinesia, and tremor. Complete loss of function leads to onset in infancy, delayed in some cases until adolescence when there is partial loss of function (Kurian, 1993; Kurian et al., 2011; Ng et al., 2014). DAT deficiency is a rare disorder, but believed to be underdiagnosed (Ng et al., 2014), and there is no effective therapy. DAT coding variants have been associated with attention-deficit/hyperactivity disorder (ADHD) (Mazei-Robison et al., 2005), and polymorphisms in the DAT gene (SLC6A3) have been associated with treatment-resistant schizophrenia (Bilic et al., 2014). Loss-of-function mutation of the DAT gene in mice (Gainetdinov et al., 1998; Giros et al., 1996) and *Drosophila* (Asjad et al., 2017) causes hyperlocomotion and disordered sleep. In mice, this is associated with reduced levels of releasable dopamine and prolongation of its clearance from the extracellular space (Gainetdinov et al., 1998). DAT-mutant mice have been used as models for ADHD and schizophrenia because of the genetic associations, behaviors, and responses to pharmacological agents (Powell et al., 2008).

We find here that zebrafish with mutation of the gene encoding DAT (*slc6a3*) hover near the bottom of the tank. We find loss of tyrosine hydroxylase (TH)-immunoreactive neurons, specifically in the A8 midbrain region of the mutant fish. The atypical antipsychotic clozapine, functioning in part through blocking of D2 receptors, reverses the behavioral defect and restores neuronal integrity in the A8 region. RNA sequencing (RNA-seq) analysis indicates that clozapine increases the expression of erythropoietin pathway genes, and transgenic over-expression of Epoa partially rescues the behavior. This suggests that the clozapine function in DAT-mutant fish is at least in part due to the restoration of midbrain TH+ neurons and that it may do so at least in part by upregulating erythropoietin expression.

RESULTS

Fish with Dopamine Transporter Deficiency Display Repetitive Bottom Swimming Behavior

We generated two independent alleles of *slc6a3*−/− using CRISPR/Cas9 technology (Figures 1A and S1, Table 1). Both cause a predicted frameshift and early termination of protein translation (Figure S1). In addition, allele 1, carrying 7-bp deletion in exon10, has markedly reduced *slc6a3* mRNA, presumably from nonsense-mediated mRNA decay (Figure 1B, Table 2). Beginning around 6 weeks post fertilization, *slc6a3*−/− fish adopt a posture with their bodies at an angle pointing toward the tank bottom (Figures 1C–1E, Videos S1, S2, and S3) and hover toward the bottom of the tank consistently, rarely leaving the lower

[1]Novartis Institutes for BioMedical Research, Cambridge, MA 02139, USA

[2]Department of Stem Cell and Regenerative Biology, Harvard University, Cambridge, MA 02138, USA

[3]Lead Contact

*Correspondence: mark_fishman@harvard.edu

https://doi.org/10.1016/j.isci.2019.06.039

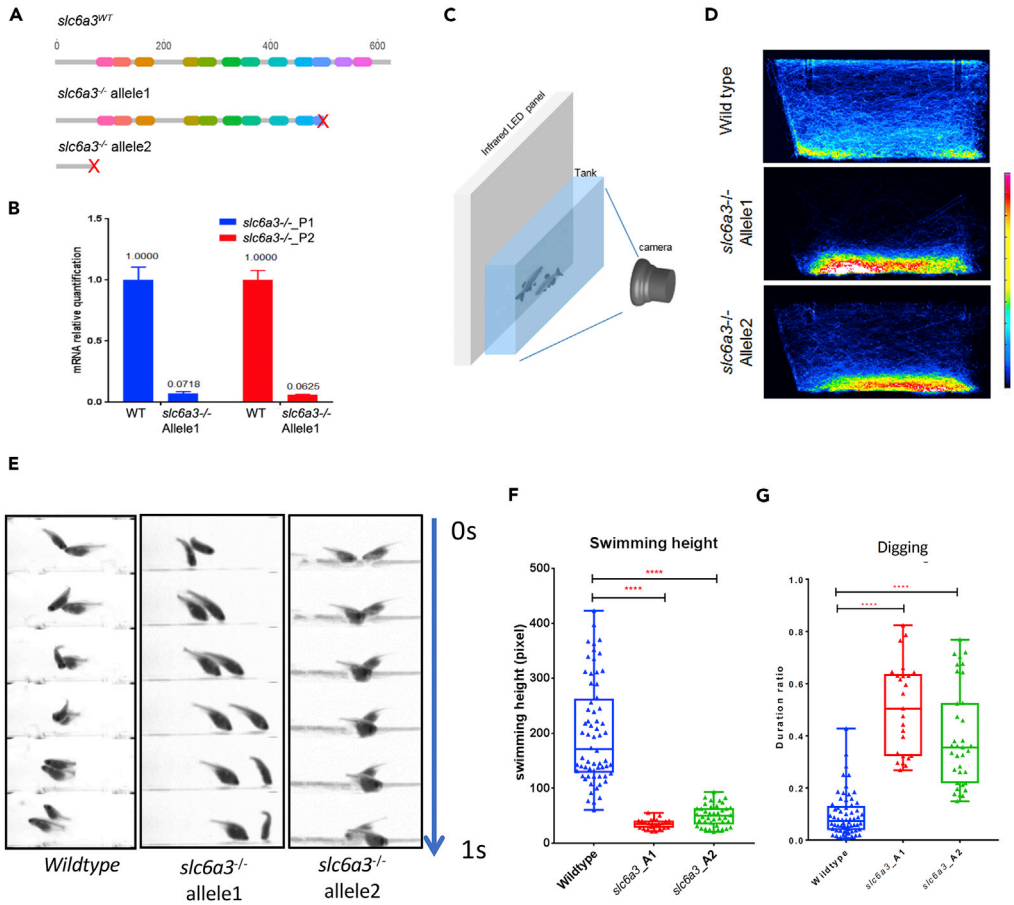

Figure 1. *slc6a3* Deficiency Causes Repetitive Behavior

(A) The wild-type *Slc6a3* protein structure and two different alleles obtained by CRISPR deletions resulting in truncation at different domains in *Slc6a3* proteins.

(B) qPCR indicating dramatic reduction of *slc6a3* truncated mRNA in *slc6a3−/−* allele1 when compared with the wild-type.

(C) The behavior recording system.

(D) Heatmaps of fish trajectory of wild-type and two alleles of *slc6a3−/−* in the home tank in a 30-min video (60 frames per second). The heatmap colors represent frames that fish appear within each 5 × 5-pixel bin in the image (1224 × 500 pixel in 30 min).

(E) The "digging" behavior in the *slc6a3−/−* fish compared with wild-type. All 1-s videos show fish at the tank bottom. Fish bearing both *slc6a3−/−* alleles display a persistent "digging" behavior, whereas wild-type fish do not.

(F) The quantification of average swimming height of fish (n_{WT} = 64, n_{slc6a3_A1} = 25, n_{slc6a3_A2} = 40, ****$p < 0.0001$, significance test: one-way ANOVA Kruskal-Wallis test).

(G) The quantification of duration of "digging" feature over the whole 30-min recording time in the tank using Janelia Automatic Animal Behavior Annotator (JABBA) (Kabra et al., 2013) (n_{WT} = 64, n_{slc6a3_A1} = 25, n_{slc6a3_A2} = 40, ****$p < 0.0001$, significance test: one-way ANOVA Kruskal-Wallis test.)

See Figure S3 for more details.

part of the tank (Figures 1E–1G), although they are fully capable of swimming toward the top of the tank to garner food (data not shown). The fish move back and forth from the bottom of the tank, a behavior reminiscent of the "digging" described previously by Tinbergen and Schemmel in other fish species (Schemmel, 1980; Tinbergen, 1952). The *slc6a3−/−* fish have normal swimming capability, although the allele2 fish manifest a slight reduction of swimming speed compared with the wild-type (Figure S3A). The tendency for *slc6a3−/−* fish to dwell toward the bottom of the tank has recently been reported by others (Kacprzak et al., 2017). The *slc6a3−/−* fish otherwise are indistinguishable from wild-type in terms of morphology, size, and development (Figure S2). Both alleles manifest reduction of spawning rates compared with wild-type: 72% (78 of 109 trials), *slc6a3−/− allele 1*: 38% (26 of 68 trials), *slc6a3−/− allele2*: 42% (10 of 24 trials).

	Allele1	Allele2
gRNA	GGAGTACTAATTGAGGCCATCGG	CGTTGAGGTCGGAGCAGTTTGGG
Genotyping primer F	GGAGTACTAATTGAGGCCATCGG	CCTTCCCAGACGTCTTCACTCCT
Genotyping primer R	ACTTGGGGAAATGTTCATCGTAGG	GATCCTGATCTCGCTGTATGTGG

Table 1. gRNAs and Genotyping Primers for *slc6a3*−/− CRISPR Knockout

Midbrain Dopaminergic Neurons Degenerate in *slc6a3*−/− Fish

slc6a3 is expressed in the brain in the diencephalon, olfactory bulb, and pretectum (Filippi et al., 2010, and Figure S5A) in larvae and adult. Brain concentrations of dopamine in the *slc6a3*−/− fish are decreased by 16% compared with wild-type (*slc6a3*−/− *allele1*: 0.024 ± 0.001 nmol/mg tissue, wild-type: 0.030 ± 0.001 nmol/mg tissue) (Figure 2E). We therefore wondered if this decline in dopamine might reflect loss or dysfunction of dopaminergic neurons and so labeled cells for TH by immunohistochemistry. As a rate-limiting enzyme of dopamine biosynthesis, TH is often used as a marker for dopaminergic neurons (Wulle and Schnitzer, 1989). We used the CUBIC clearing strategy to visualize TH+ neurons throughout the entire adult brain (Susaki et al., 2015). We find, as have others (Parker et al., 2013), that TH+ neurons are concentrated in a few discrete clusters (Figures 2A and S5B). *slc6a3* mutation causes reduction of TH+ neuron number and branching pattern, primarily limited to the midbrain areas termed A8 and A9 in 8-week-old fish brains (Figures 2B–2D, 2C′–D′, 2F, and S5C). TH+ neuron loss in other brain areas was not detected (Figure S5D). The A8 region of the zebrafish midbrain is believed to be homologous to the retrorubral field (RrF) region of mammals, and the A9 region, to the substantia nigra (SNc) (German and Manaye, 1993).

Chronic Treatment with Clozapine Rescues Wild-Type Behavior and Midbrain TH+ Neurons

We screened psychoactive compounds, especially those known to act at least in part by affecting dopamine signaling, upon the bottom-dwelling behavior of *slc6a3*−/− fish. We chose doses predicted to achieve, at final dilution in the water, concentrations of 1× or 5× the EC50 for dopamine receptors and assessed swimming behaviors over time (Figure 3A). Of the compounds, clozapine has the clearest effect on swimming behavior, although it takes at least 3 weeks to manifest (Figures 3B–3D). As shown in Figure 3C, clozapine exposure for 3 weeks causes the fish to resume swimming throughout the height of the tank and, as shown in the attached videos (Videos S4 and S5), completely abrogates the repetitive "digging" behavior (Figures 3D and S4). Thus, clozapine effectively restores the *slc6a3*−/− behaviors to wild-type.

We also find that 3 weeks of exposure to 2.5 μM clozapine treatment rescues A8 (but not A9) TH+ neuronal number and morphology (3 months post-fertilization, Figures 3E–F′, 3E′–3F′, 3G, and S5E–S5H). This is compatible with the A8 regional loss contributing to the unusual behavior of the mutant fish and suggests that clozapine may act, at least in part, by protecting this population of cells.

Erythropoietin Pathway as a Potential Clozapine Target

To begin to dissect pathways by which clozapine rescues the *slc6a3*−/− behavior we performed RNA-seq of the adult *slc6a3*−/− fish brains and compared clozapine with control treatment (Table S1). Interestingly, levels of dopamine pathway genes are only modestly affected by clozapine treatment (Figure S6A). The most significant changes in expression are in *erythropoietin a* (*epoa*, by 6.35 ± 1.62-fold) and *5′-nucleotidase, cytosolic II, like 1* (*nt5c2l1* by 5.73 ± 0.69-fold) (Figures 4A and 4B), the latter an enzyme that converts extracellular nucleotides, such as 5′-AMP, to nucleotides, such as adenosine. There are also significant increases in expression of *erythropoietin receptor* (*epor*, by 1.92 ± 0.54-fold) (Figures 4A and 4B). Quantitative RT-PCR of these genes independently confirmed the upregulation by clozapine (Figure S6B, Table 2). We focused on the *epo* pathway because erythropoietin has been previously reported to have neuroprotective effects, particularly on midbrain dopaminergic neurons (Noguchi et al., 2007; Punnonen et al., 2015). We generated a transgenic line stably expressing *epoa* in CNS neurons (driven by a neuronal alpha tubulin promoter, Figures 4C–4E), and which increases *epoa* expression levels by more than 2-fold (Figure 4F). When crossed into *slc6a3*−/− fish, their behavior was restored toward wild-type (Figures 4G and 4H, Video S6), indicating that the clozapine-induced *epoa* expression may account for part of clozapine's effect in these fish.

	Forward	Reverse
slc6a3-Q1	GGTTCAGTTCACCTCCTCCA	ACGGACAGCAGAAAGTCGAT
slc6a3-Q2	CCTTCCTCATCTCGCTCATC	TCATCACTGAAGCGATCCAC
epoa	TGATGAAGCTTGTCCAGCAC	CAGCTTCCGAGAAAAACCTG
epor	GAGGACCAGCGTTCAGACTC	GTGCGAGGCATTTAGAGAGG
nt5c2l1	TGGCGCTCTTACTTTGACCT	CCTGTCGCTTCTTGGACTTC
bactin	CGAGCAGGAGATGGGAAC	CAACGGAAACGCTCATTGC

Table 2. Sequences of qRT-PCR Primers

DISCUSSION

We find that homozygous loss of the dopamine uptake transporter, DAT (SLC6A3), causes zebrafish to manifest an unusual repetitive bottom-digging behavior, one reminiscent of sand digging of threatened sticklebacks (Tinbergen, 1952) and bottom searching by cave fish (*Astyanax mexicanus*) (Schemmel, 1980). Thus, it may be part of a piscine behavioral repertoire, one exaggerated in zebrafish by the mutation. The behavior is accompanied by loss of particular set of midbrain TH+ neurons. Clozapine, an atypical antipsychotic, can restore wild-type behavior and neuronal morphology in one group of the TH neurons. Clozapine increases the expression of erythropoietin pathway genes, and transgenic over-expression of erythropoietin in neurons of *slc6a3−/−* fish can partially substitute for clozapine in restoring normal behavior.

DAT activity is the primary mechanism for ending dopaminergic transmission, keeping extracellular dopamine levels low, and restoring presynaptic levels. Genetic evidence indicates a role for DAT in both motor and cognitive functions. DAT is the target of the psychostimulants cocaine and amphetamine. In humans, complete loss of function of DAT in humans leads to infantile Parkinson disease, and partial loss, to late-onset dyskinesia (Kurian, 1993; Kurian et al., 2011). DAT polymorphisms or changes in expression levels have been associated with several psychiatric and neurological disorders, including schizophrenia, ADHD, psychostimulant abuse, and Gilles de las Tourette syndrome (Kurian, 1993; Kurian et al., 2011).

We noted no gross morphological change in the *slc6a3−/−* brain. This is consistent with the MRI scan in patients with DAT deficiency syndrome (Ng et al., 2014). The most prominent effect we noted in the *slc6a3−/−* fish is neuronal loss and dysmorphology of TH-expressing neurons primarily in the A8 and A9 regions of the midbrain. These are believed to be homologous to RrF and SNc regions of the mammalian brain, respectively (Arenas et al., 2015; Parker et al., 2013). TH+ neurons of the SNc project to the caudate putamen and dorsolateral striatum, and their loss in Parkinson disease is believed to be responsible for the gait abnormalities in this disorder (Arenas et al., 2015). The TH+ neurons of the A8 homologous region, the RrF, project to the nucleus accumbens and the limbic cerebral cortex and have been proposed to be involved in emotion, reward, and cognitive function, and to be affected in a range of psychiatric disorders (Arenas et al., 2015; Gallo et al., 2018). Abnormalities of both the nucleus accumbens and limbic cerebral cortex are implicated in schizophrenia pathology by postmortem human tissue analysis (Jakob and Beckmann, 1986; McCollum and Roberts, 2015). Interestingly, *slc6a3*-mutant mice manifest only minor reductions in TH-immunoreactive neurons in the striatum, the region most affected (Cyr et al., 2003). This may reflect a species difference, or it may be that, as in the fish, it is only a small subpopulation of specific neurons that are lost in the mouse.

Clozapine was synthesized originally with the goal of avoiding the extrapyramidal side effects of earlier antipsychotic drugs, assumed accomplished by diminishing its D2 activity. However, it is clear that its therapeutic mechanism is unlikely to be explained solely by its effect upon the dopamine system, because it also enhances the activity at serotonin 2A receptor and several other receptors (Crilly, 2007). Clozapine's use is compromised by rare but life-threatening agranulocytosis, and more common weight gain, so understanding its mechanism of action is critical to the development of efficacious and safer therapeutics. The zebrafish brain can regenerate neurons in response to injury (Fleisch et al., 2011; Ghosh and Hui, 2016), and it is certainly conceivable that human responses to clozapine might not include the dramatic repair that we see here.

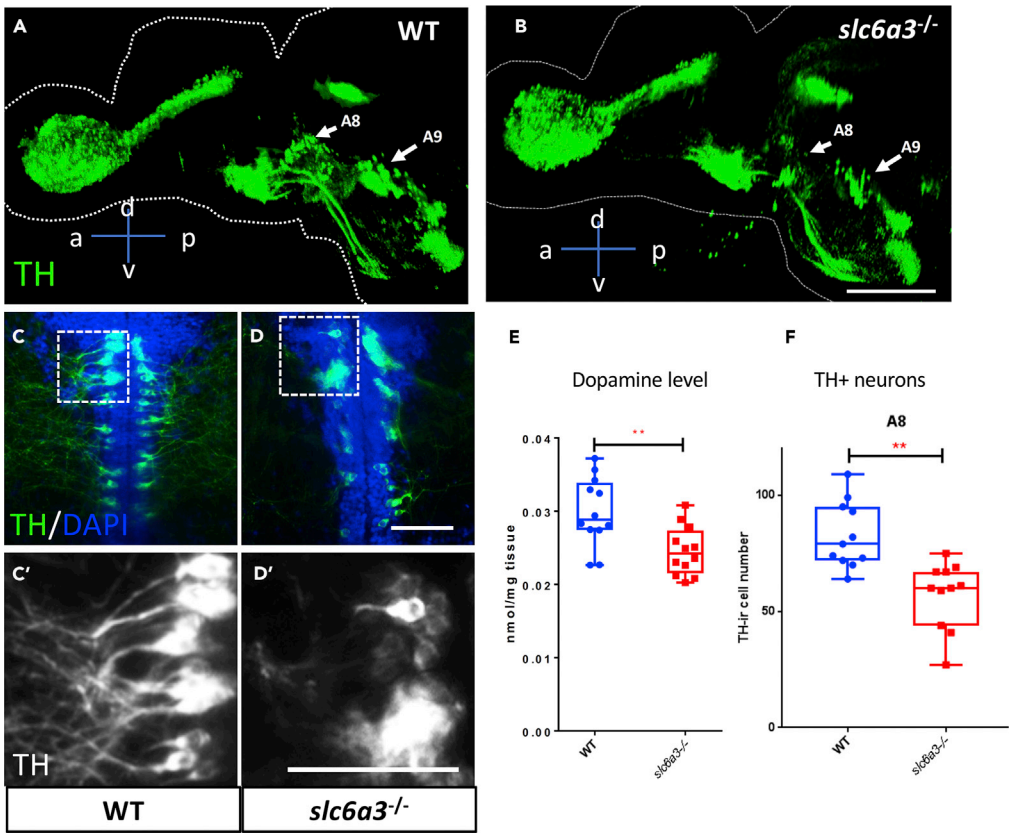

Figure 2. Midbrain Tyrosine Hydroxylase Immunoreactive (TH+) Neurons Degenerate in the *slc6a3*−/− Fish Brain

(A and B) Sagittal view of 3-dimensional rendering of tyrosine hydroxylase (TH) immunostaining of the whole brains of (A) wild-type (WT) and (B) *slc6a3*−/− *allelle1* at 3 months post-fertilization. The arrows indicate two groups of TH+ neurons (A8 and A9 areas) in the midbrain and show reduction in cell numbers in the *slc6a3*−/− *allele1* compared with WT. Scale bar, 400 μm. a, anterior; p, posterior; d, dorsal; v, ventral.

(C–E) (C and D) Representative images of TH+ neurons in (C and C′) WT and (D and D′) *slc6a3*−/− *allele1* fish brain in the A8 area at 2 months post-fertilization showing structural changes in neurons and diminution in their arborization. For visualization purpose, images are shown as horizontal ventral views, with anterior on the top. Five optical planes (6-μm interval) were stacked to show the TH+ cells. Scale bar, 20 μm. (E) Mass spectrometry of the dopamine level shows a significant reduction in the *slc6a3*−/− fish. n = 12 for both WT and *slc6a3*−/− *allele1*. **p < 0.01. Significance test: Wilcoxon-Mann-Whitney test.

(F) Boxplot shows reduction in cell numbers of A8 TH+ neurons at 2 months post-fertilization.

Error bar = standard deviation. n = 11 for both WT and *slc6a3*−/− allele1. **p < 0.01. Significance test: Wilcoxon-Mann-Whitney test.

We find that *epoa* and *epo* receptors are among the genes whose expressions are most increased by clozapine and that transgenic *epoa* expression in neurons can mirror clozapine's restorative effect on behavior. These observations are of interest because, in addition to its well-defined role in erythropoiesis, the Epo pathway has been proposed as neuroprotective in a variety of CNS disorders, including ischemia, traumatic brain injury, Parkinson disease, and schizophrenia (Kastner et al., 2012; Punnonen et al., 2015). In the CNS, EpoRs are expressed by neurons, glia, and endothelial cells, especially during embryonic development (Noguchi et al., 2007). Mice lacking Epo or its receptor have defective neurogenesis during development (Noguchi et al., 2007). Adult TH+ neurons express EpoR, and Epo can rescue neurons from 6-hydroxydopamine toxicity, both *in vitro* and *in vivo* by CNS infusion (Punnonen et al., 2015). It is believed that Epo actions in the CNS are mediated by a heterodimer of the EpoR and CD131, rather than via the homodimer responsible for Epo activation of erythropoiesis (Punnonen et al., 2015). Mutation of *slc6a3* does not by itself affect *epoa* levels, so we presume that Epo is not in the pathway directly affected by *slc6a3* mutation and that salvage by transgenic over-expression of Epo is likely to act by a pathway parallel to that perturbed in *slc6a3*−/− fish.

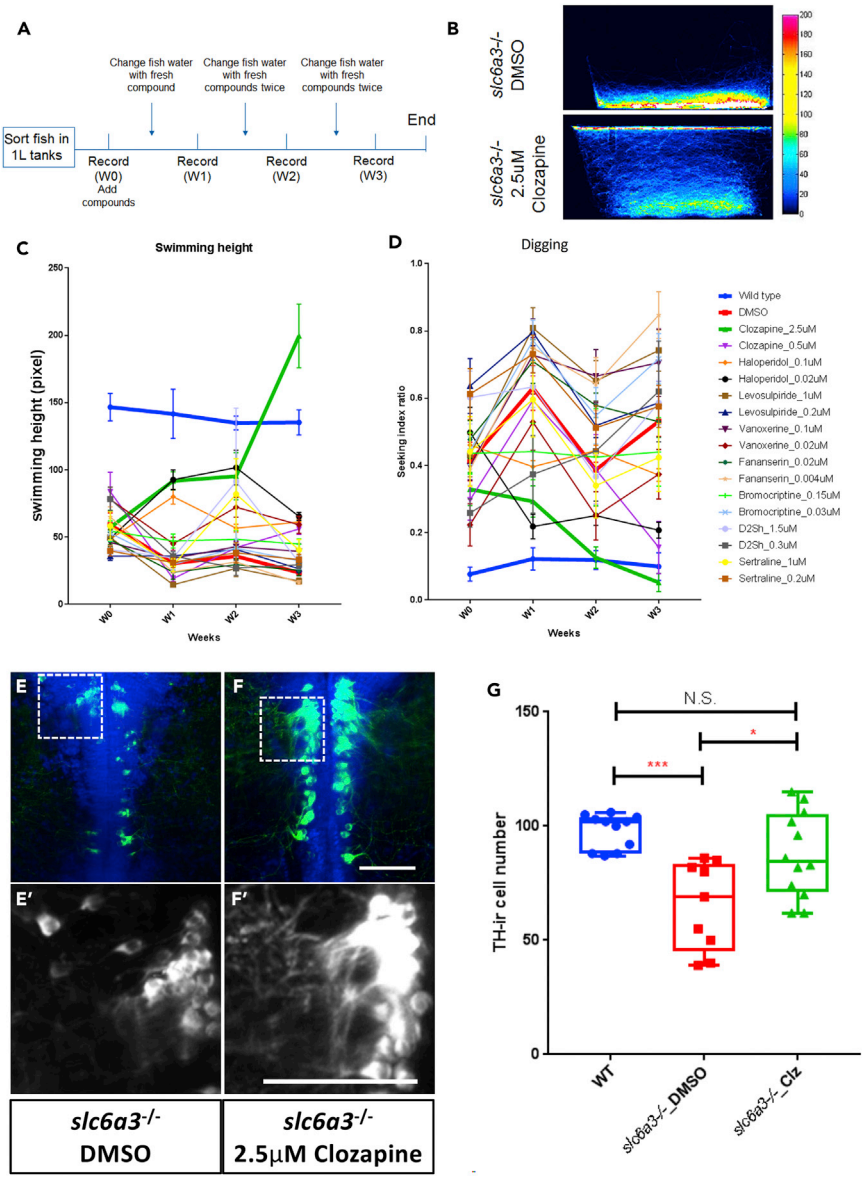

Figure 3. Chronic Clozapine Treatment Rescues Aberrant Swimming Behavior and Midbrain TH+ Neurons in the *slc6a3−/−* Fish Brain

(A) Schematic of the experimental design for chronic treatment of *slc6a3−/−* allele1 mutant fish with candidate compounds.

(B) The heatmap of fish trajectories of control (DMSO) and 2.5 μM clozapine-treated *slc6a3−/−* allele1 fish after 3 weeks' treatment showing that clozapine reverses aberrant "digging" behavior.

(C) Time course of swimming height from week 0 (W0) to week 3 (W3) (n = 5; error bar = standard deviation).

(D) The time course of the "digging" feature duration by all compounds over time (n = 5, error bar = standard deviation).

(E–F) Representative images of TH+ neurons in (E and E′) DMSO and (F and F′) 2.5 μM clozapine-treated *slc6a3−/− allele1* fish brain in the A8 area at 3 months post-fertilization showing restoration of neuronal number and arborization by clozapine. For visualization purpose, images are shown as horizontal ventral views, with anterior on the top. Five optical planes (6-μm interval) were stacked to show the TH+ cells. Scale bar, 20 μm.

(G) Boxplot shows clozapine-induced restoration of TH-immunoreactive A8 cell number in *slc6a3−/− allele1* fish at 3 months post-fertilization.

(For all, n ≥10. Error bar = standard deviation. ***p < 0.001, *p < 0.05. N.S., no significance. Significance test: one-way ANOVA Kruskal-Wallis test).

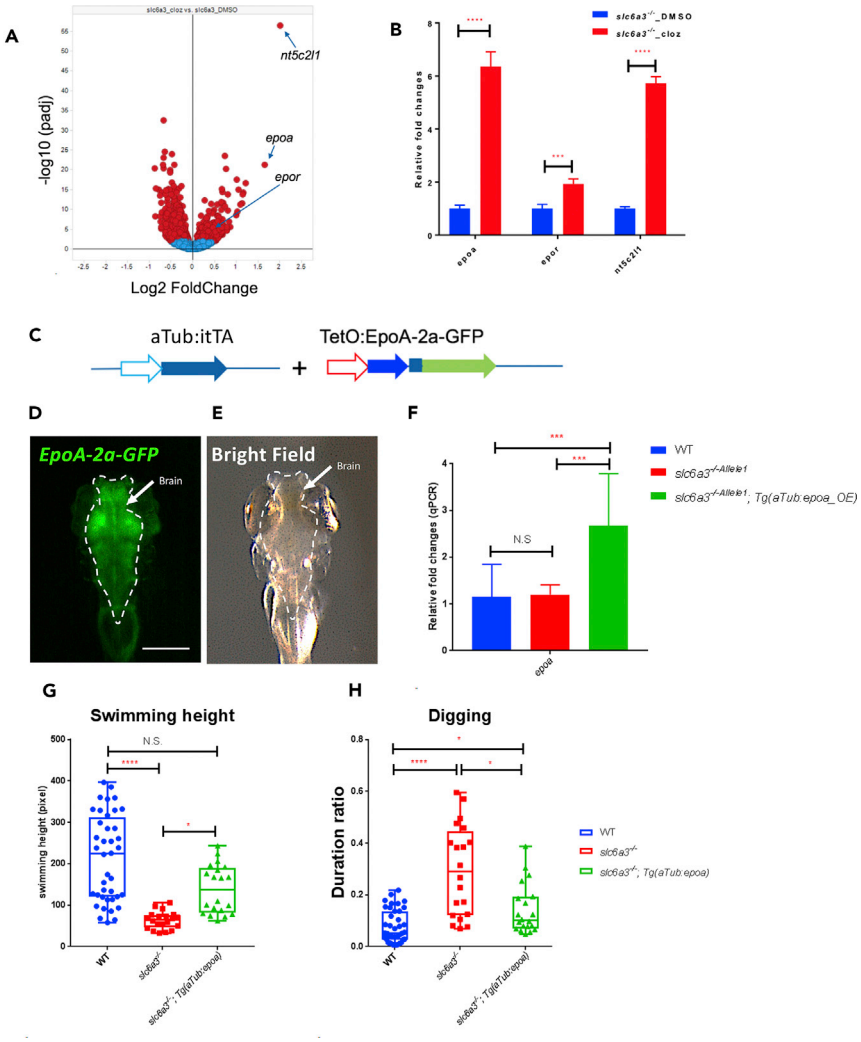

Figure 4. RNA-Seq Analysis Reveals Erythropoietin Pathway as a Potential Clozapine Target

(A) The volcano plot of log2-fold change of gene expression in the adult fish brain between the treatments of clozapine and DMSO in *slc6a3−/− allele1*. The clozapine highly upregulated genes (*epoa*, *epor*, and *nt5c2l1*) are indicated on the graph.

(B) Bar plot of gene expression of *epoa*, *epor*, and *nt5c2l1* by RNA-seq analysis. ****p < 0.0001, ***p < 0.001. n = 8 for all. Error bar = standard deviation. Significance test: Wilcoxon-Mann-Whitney test.

(C) The construct maps for over-expression of *epoa* in neurons with the tetracycline-controlled transcriptional activation system.

(D and E) The dorsal view of the green channel (D) and bright field (E) of a *slc6a3*$^{-/-\_allele1}$*; Tg(aTub:iTTA; TetO:EpoA-2a-GFP)* fish at 5 days post-fertilization under a fluorescent dissecting microscope. The brain area (indicated by green fluorescence in D) is outlined by a dotted line. Scale bar, 250 μm.

(F) Whole-brain qRT-PCR at 2 months post-fertilization confirms the upregulation of *epoa* in the *slc6a3*$^{-/-\_allele1}$*;Tg*(*aTub:iTTA*; *TetO:EpoA-2a-GFP*) fish. Error bar, standard deviation. n = 6 for all conditions. ***p < 0.001, **p < 0.01, N.S., no significance. Significance test, Wilcoxon-Mann-Whitney test.

(G and H) The quantification of The quantification of average swimming height (G) and duration of "digging" feature (H) of *slc6a3*$^{-/-\_allele1}$*; Tg*(*aTub:iTTA*; *TetO:EpoA-2a-GFP*) compared to *slc6a3*$^{-/-\_allele1}$ and wild-type at 2 months post-fertilization. n_{WT} = 40, $n_{slc6a3-/-\_allele1\_}$ = 20, $n_{slc6a3-/-\_allele1;\ tg(aTub:eopa)}$ = 20. ****p < 0.0001, *p < 0.05, N.S., no significance. Significance test: one-way ANOVA Kruskal-Wallis test.

We speculate that damage to TH+ neurons in the A8 (and A9) region of the zebrafish midbrain is responsible for the bottom-digging-like repetitive behavior of the *slc6a3−/−* fish, and that clozapine rescue of the A8 neural cells is responsible for restoring their behavior toward that of wild-type. Interestingly, we do not see significant rescue of A9 by clozapine treatment. Of course, we cannot determine whether the rescue of TH+ neurons also accounts for clozapine's therapeutic effect in humans,

although the areas perturbed in schizophrenia include those believed homologous to projection zones of A8-equivalent (i.e., RrF) DA neurons. In addition, the similar restorative effect exerted by erythropoietin expression suggests that this might be a novel pathway to explore for discovery of new medicines with clozapine-like therapeutic activities.

Limitations of the Study

The observations suggest that the behavioral disorder may be due to A8 neuronal dysfunction, but proof will require specific targeting of such neurons, unfortunately technically non-trivial because the midbrain is relatively deep in animals old enough to manifest this behavioral phenotype.

We have focused upon the Epo pathway as one potential intermediary in the clozapine effect. Transgenic *epoa* expression rescues behavior in *slc6a3−/−* animals, but not to the same degree as clozapine, suggesting that we may need to target more precisely or that it explains only part of clozapine's effect. Along these lines it would be of interest to mutate *epoa* to see if such mutation generates behavior akin to that seen in *slc6a3−/−* fish, but the critical role of Epo in hematopoiesis causes early death in such animals. Genes other than *epoa* are regulated by clozapine and could be important. For example, there is an increase in 5′-nucleotidase (an enzyme that converts extracellular nucleotides, such as 5′-AMP, to nucleotide, such as adenosine), the activity of which is known to increase after clozapine treatment in humans and in the rat (Brunstein et al., 2007; Lara et al., 2001).

METHODS

All methods can be found in the accompanying Transparent Methods supplemental file.

SUPPLEMENTAL INFORMATION

Supplemental Information can be found online at https://doi.org/10.1016/j.isci.2019.06.039.

ACKNOWLEDGMENTS

We thank Ajeet Singh, Alexis Hubaud, and Jian Fang for helpful discussions and scientific input on the manuscripts. We thank Stephanie Wiessner, Gregory Molind, Ellen Sanchez, Carmen Diaz Verdugo, Jingyao Li, and Wenlong Tang for helpful discussions and help with reagents and hardware. We thank Ned Kirkpatrick and Novartis Imaging Core for helping with microscopy, Carsten Russ and Novartis NGS facility for sequencing, and Kara Maloney and Novartis zebrafish facility for animal care.

AUTHOR CONTRIBUTIONS

G.W., P.Z., and M.C.F. conceived the project; G.W., G.Z., D.J.G., and M.C.F. designed experiments; G.W., Z.L., and C.H.F. performed most of the experiments; G.Z., Z.L., and M.C. generated the mutant alleles; G.W. and C.H.F. performed immunofluorescence imaging and data analysis; G.W., G.Z., Z.L., and M.X.S. performed the RNA-seq experiment and data analysis; G.W. and Z.L. generated overexpression constructs and performed injection; G.W. and T.T. performed behavior data acquisition and analysis; K.M. and S.J.T. performed mass spectrometry experiment and analysis; P.Z., D.J.G., and M.C.F. supervised the project; G.W., D.J.G., and M.C.F. wrote the paper with input from all authors.

DECLARATION OF INTERESTS

M.C.F. is an advisor to Novartis, MPM, and Burrage Capital and member of the Board of Directors of Semma Therapeutics and Beam Therapeutics, and of the SAB of Tenaya Therapeutics. All other authors were Novartis employees at the time study was conducted. D.J.G. is an employee of and stockholder in Novartis. This study was funded by Novartis AG.

Received: March 8, 2019
Revised: May 17, 2019
Accepted: June 28, 2019
Published: July 26, 2019

REFERENCES

Arenas, E., Denham, M., and Villaescusa, J.C. (2015). How to make a midbrain dopaminergic neuron. Development *142*, 1918–1936.

Asjad, H.M.M., Kasture, A., El-Kasaby, A., Sackel, M., Hummel, T., Freissmuth, M., and Sucic, S. (2017). Pharmacochaperoning in a Drosophila model system rescues human dopamine transporter variants associated with infantile/juvenile parkinsonism. J. Biol. Chem. *292*, 19250–19265.

Bilic, P., Jukic, V., Vilibic, M., Savic, A., and Bozina, N. (2014). Treatment-resistant schizophrenia and DAT and SERT polymorphisms. Gene *543*, 125–132.

Brunstein, M.G., Silveira, E.M., Jr., Chaves, L.S., Machado, H., Schenkel, O., Belmonte-de-Abreu, P., Souza, D.O., and Lara, D.R. (2007). Increased serum adenosine deaminase activity in schizophrenic receiving antipsychotic treatment. Neurosci. Lett. *414*, 61–64.

Crilly, J. (2007). The history of clozapine and its emergence in the US market: a review and analysis. Hist. Psychiatry *18*, 39–60.

Cyr, M., Beaulieu, J.M., Laakso, A., Sotnikova, T.D., Yao, W.D., Bohn, L.M., Gainetdinov, R.R., and Caron, M.G. (2003). Sustained elevation of extracellular dopamine causes motor dysfunction and selective degeneration of striatal GABAergic neurons. Proc. Natl. Acad. Sci. U S A *100*, 11035–11040.

Filippi, A., Mahler, J., Schweitzer, J., and Driever, W. (2010). Expression of the paralogous tyrosine hydroxylase encoding genes th1 and th2 reveals the full complement of dopaminergic and noradrenergic neurons in zebrafish larval and juvenile brain. J. Comp. Neurol. *518*, 423–438.

Fleisch, V.C., Fraser, B., and Allison, W.T. (2011). Investigating regeneration and functional integration of CNS neurons: lessons from zebrafish genetics and other fish species. Biochim. Biophys. Acta *1812*, 364–380.

Gainetdinov, R.R., Jones, S.R., Fumagalli, F., Wightman, R.M., and Caron, M.G. (1998). Re-evaluation of the role of the dopamine transporter in dopamine system homeostasis. Brain Res. Brain Res. Rev. *26*, 148–153.

Gallo, E.F., Meszaros, J., Sherman, J.D., Chohan, M.O., Teboul, E., Choi, C.S., Moore, H., Javitch, J.A., and Kellendonk, C. (2018). Accumbens dopamine D2 receptors increase motivation by decreasing inhibitory transmission to the ventral pallidum. Nat. Commun. *9*, 1086.

German, D.C., and Manaye, K.F. (1993). Midbrain dopaminergic neurons (nuclei A8, A9, and A10): three-dimensional reconstruction in the rat. J. Comp. Neurol. *331*, 297–309.

Ghosh, S., and Hui, S.P. (2016). Regeneration of zebrafish CNS: adult neurogenesis. Neural Plast. *2016*, 5815439.

Giros, B., Jaber, M., Jones, S.R., Wightman, R.M., and Caron, M.G. (1996). Hyperlocomotion and indifference to cocaine and amphetamine in mice lacking the dopamine transporter. Nature *379*, 606–612.

Jakob, H., and Beckmann, H. (1986). Prenatal developmental disturbances in the limbic allocortex in schizophrenics. J. Neural Transm. *65*, 303–326.

Kabra, M., Robie, A.A., Rivera-Alba, M., Branson, S., and Branson, K. (2013). JAABA: interactive machine learning for automatic annotation of animal behavior. Nat. Methods *10*, 64–67.

Kacprzak, V., Patel, N.A., Riley, E., Yu, L., Yeh, J.J., and Zhdanova, I.V. (2017). Dopaminergic control of anxiety in young and aged zebrafish. Pharmacol. Biochem. Behav. *157*, 1–8.

Kastner, A., Grube, S., El-Kordi, A., Stepniak, B., Friedrichs, H., Sargin, D., Schwitulla, J., Begemann, M., Giegling, I., Miskowiak, K.W., et al. (2012). Common variants of the genes encoding erythropoietin and its receptor modulate cognitive performance in schizophrenia. Mol. Med. *18*, 1029–1040.

Kurian, M.A. (1993). SLC6A3-related dopamine transporter deficiency syndrome. In GeneReviews((R)), M.P. Adam, H.H. Ardinger, R.A. Pagon, S.E. Wallace, L.J.H. Bean, K. Stephens, and A. Amemiya, eds. (Seattle: University of Washington), https://www.ncbi.nlm.nih.gov/books/NBK442323/.

Kurian, M.A., Li, Y., Zhen, J., Meyer, E., Hai, N., Christen, H.J., Hoffmann, G.F., Jardine, P., von Moers, A., Mordekar, S.R., et al. (2011). Clinical and molecular characterisation of hereditary dopamine transporter deficiency syndrome: an observational cohort and experimental study. Lancet Neurol. *10*, 54–62.

Lara, D.R., Vianna, M.R., de Paris, F., Quevedo, J., Oses, J.P., Battastini, A.M., Sarkis, J.J., and Souza, D.O. (2001). Chronic treatment with clozapine, but not haloperidol, increases striatal ecto-5′-nucleotidase activity in rats. Neuropsychobiology *44*, 99–102.

Mazei-Robison, M.S., Couch, R.S., Shelton, R.C., Stein, M.A., and Blakely, R.D. (2005). Sequence variation in the human dopamine transporter gene in children with attention deficit hyperactivity disorder. Neuropharmacology *49*, 724–736.

McCollum, L.A., and Roberts, R.C. (2015). Uncovering the role of the nucleus accumbens in schizophrenia: a postmortem analysis of tyrosine hydroxylase and vesicular glutamate transporters. Schizophr. Res. *169*, 369–373.

Ng, J., Zhen, J., Meyer, E., Erreger, K., Li, Y., Kakar, N., Ahmad, J., Thiele, H., Kubisch, C., Rider, N.L., et al. (2014). Dopamine transporter deficiency syndrome: phenotypic spectrum from infancy to adulthood. Brain *137*, 1107–1119.

Noguchi, C.T., Asavaritikrai, P., Teng, R., and Jia, Y. (2007). Role of erythropoietin in the brain. Crit. Rev. Oncol. Hematol. *64*, 159–171.

Parker, M.O., Brock, A.J., Walton, R.T., and Brennan, C.H. (2013). The role of zebrafish (Danio rerio) in dissecting the genetics and neural circuits of executive function. Front. Neural Circuits *7*, 63.

Powell, S.B., Young, J.W., Ong, J.C., Caron, M.G., and Geyer, M.A. (2008). Atypical antipsychotics clozapine and quetiapine attenuate prepulse inhibition deficits in dopamine transporter knockout mice. Behav. Pharmacol. *19*, 562–565.

Punnonen, J., Miller, J.L., Collier, T.J., and Spencer, J.R. (2015). Agonists of the tissue-protective erythropoietin receptor in the treatment of Parkinson's disease. Curr. Top. Med. Chem. *15*, 955–969.

Schemmel, C. (1980). Studies on the genetics of feeding behaviour in the cave fish Astyanax mexicanus f. anoptichthys. An example of apparent monofactorial inheritance by polygenes. Z. Tierpsychol. *53*, 9–22.

Susaki, E.A., Tainaka, K., Perrin, D., Yukinaga, H., Kuno, A., and Ueda, H.R. (2015). Advanced CUBIC protocols for whole-brain and whole-body clearing and imaging. Nat. Protoc. *10*, 1709–1727.

Tinbergen, N. (1952). Derived activities; their causation, biological significance, origin, and emancipation during evolution. Q. Rev. Biol. *27*, 1–32.

Wulle, I., and Schnitzer, J. (1989). Distribution and morphology of tyrosine hydroxylase-immunoreactive neurons in the developing mouse retina. Brain Res. Dev. Brain Res. *48*, 59–72.

ISCI, Volume *17*

Supplemental Information

Abnormal Behavior of Zebrafish Mutant in Dopamine Transporter Is Rescued by Clozapine

Guangliang Wang, Guoqiang Zhang, Zhuyun Li, Caroline H. Fawcett, Matthew Coble, Maria X. Sosa, Tingwei Tsai, Kimberly Malesky, Stefan J. Thibodeaux, Peixin Zhu, David J. Glass, and Mark C. Fishman

Supplemental Information

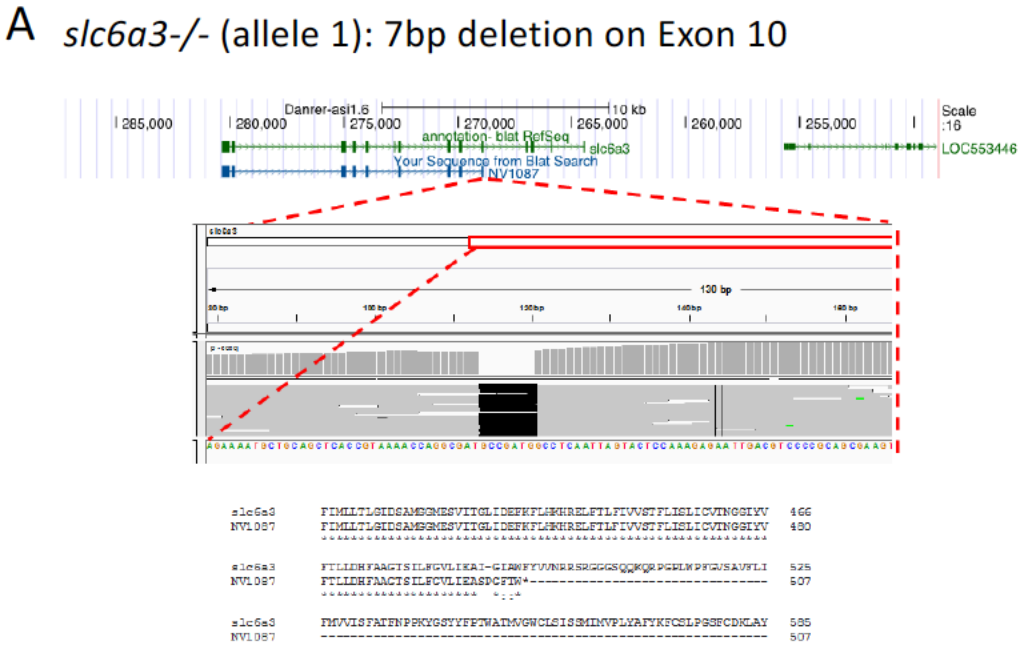

Supplementary Figure 1. Sequence confirmation of CRISPR deletions in the two *slc6a3-/-* alleles, related to Figure 1. (**A**) Mutation in *slc6a3-/-* allele1 is a 7bp deletion in Exon10. (**B**) Mutation of *slc6a3-/-* allele2 is a 4 bp deletion in Exon 3.

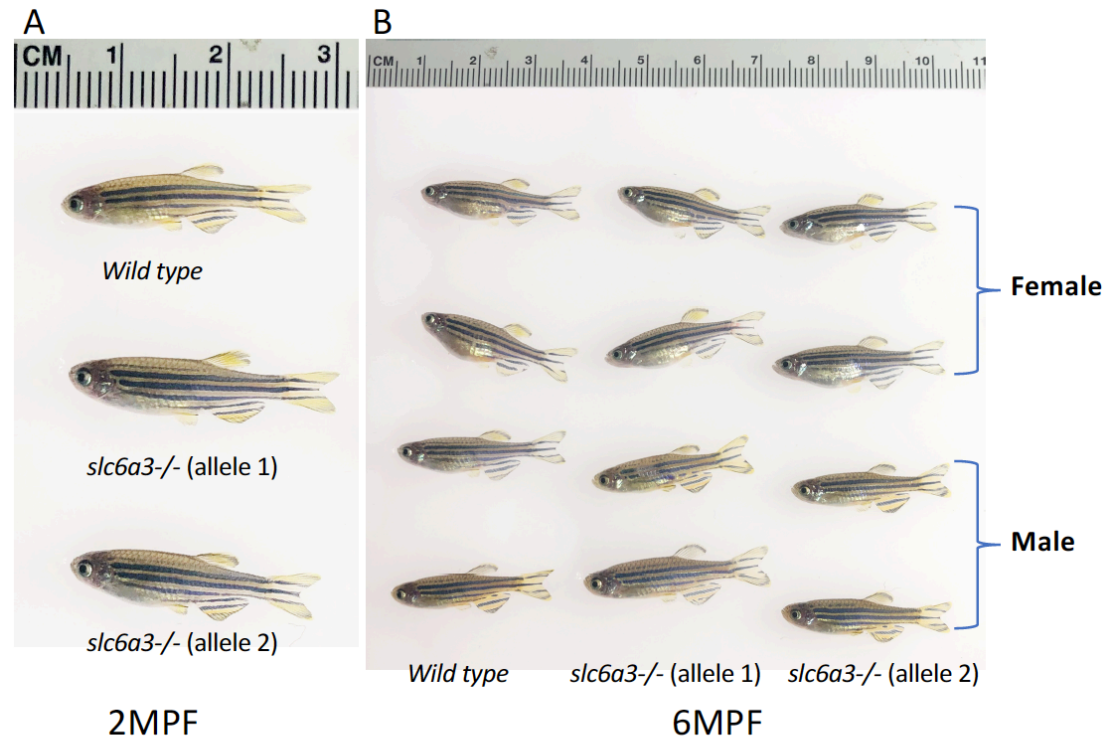

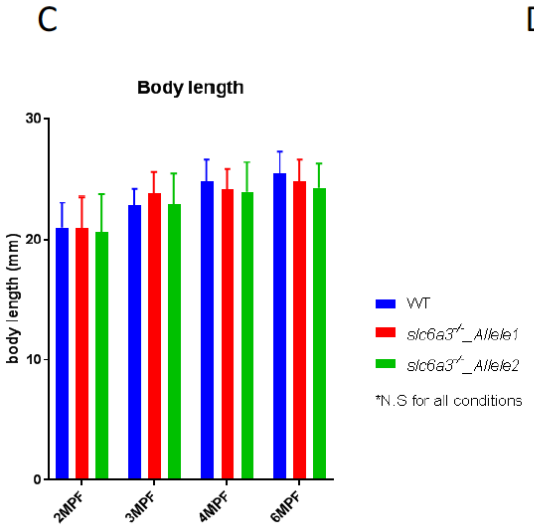

Supplementary Figure 2. *slc6a3* knockout does not affect overall morphology and development, related to Figure 1. (**A**) Zebrafish images of WT, *slc6a3-/- allele1*, and *slc6a3-/- allele2* at 2 months post-fertilization (2mpf). It should be noted that fish do not show gender-related morphology yet at this stage. (**B**) Zebrafish images of wild-type (WT), *slc6a3-/- allele1*, and *slc6a3-/- allele2* at 6 months post-fertilization (6mpf). (**C**) Fish body length (head to tail) measurement of WT, *slc6a3-/-* allele1, and *slc6a3-/- allele2* at 2mpf, 3mpf, 4mpf, and 6mpf. For all n>=16, significance test: one-way ANOVA Kruskal-Wallis test.

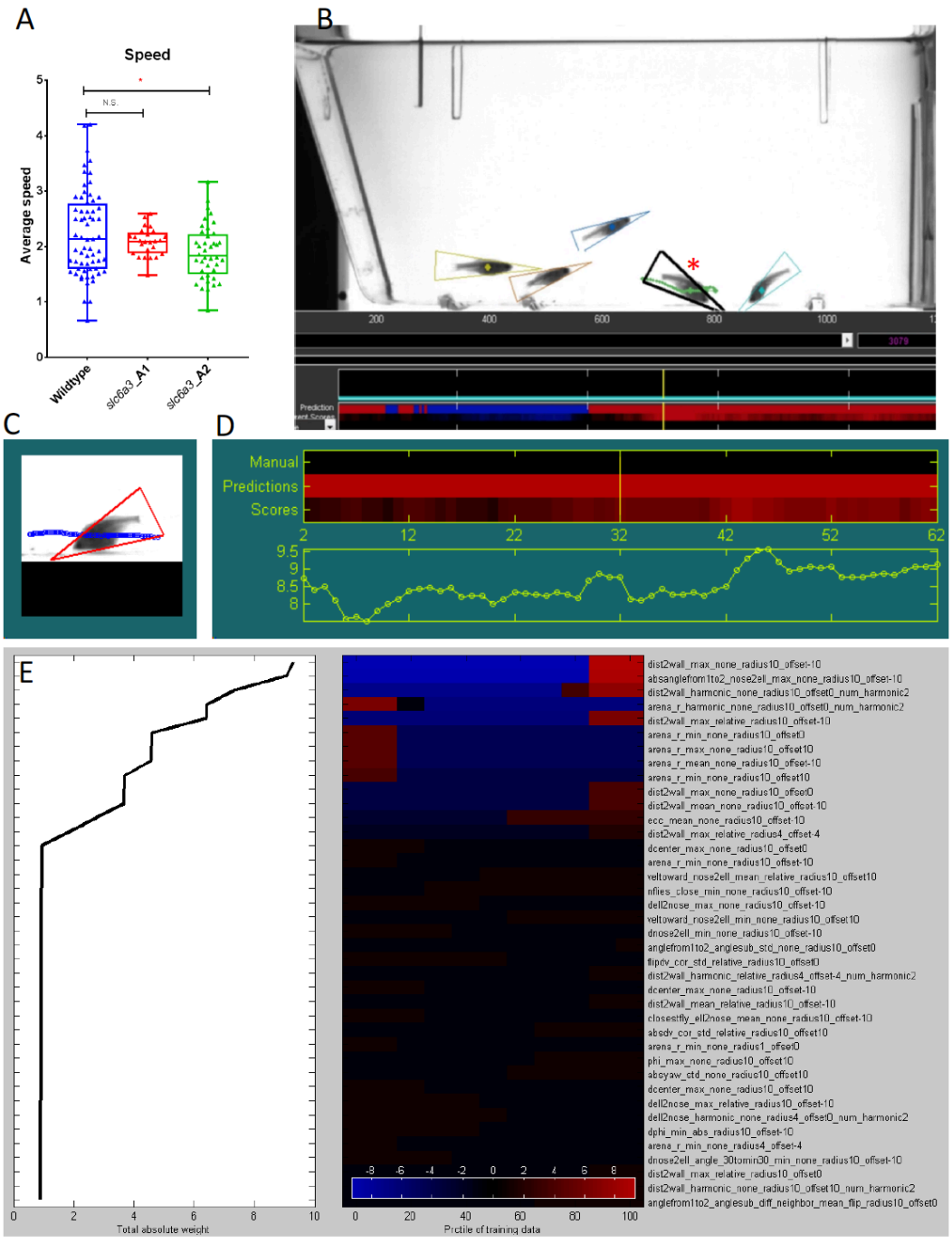

Supplementary Figure 3. Training the "digging" classifier in JABBA, related to Figure 1. (**A**) the average swimming speed of WT, *slc6a3-/- allele1*, and *slc6a3-/- allele2* (n_{WT}=64, $n_{slc6a3\text{-}/\text{-}\_A1}$=25, $n_{slc6a3\text{-}/\text{-}\_A2}$=40, *$p<0.05$, N.S.= no significance. Significance test: one-way ANOVA Kruskal-Wallis test). (**B**) The interphase of training "digging" classifier in JABBA. The fish posture is highlighted by a triangle (asterisk) with a centroid in the center of the fish. The triangle indicates the angles of fish toward to the bottom. (**C**) The view of individual fish during the

training. The blue line indicates the fish trajectory ±30 seconds of the timepoint. (**D**) The view of the "digging" label in a 60 second timeframe. Manual=manually labelled "digging" behavior (left blank here as the timeframe is randomly selected and not manually labelled). Prediction=predicted probability after training. Score=the probability score based on on all weighted features. A score of 0.75 was used for as the threshold for filtering the "digging" motif in video. (**E**) The rank of total absolute weights of all features for training the "digging" classifier.

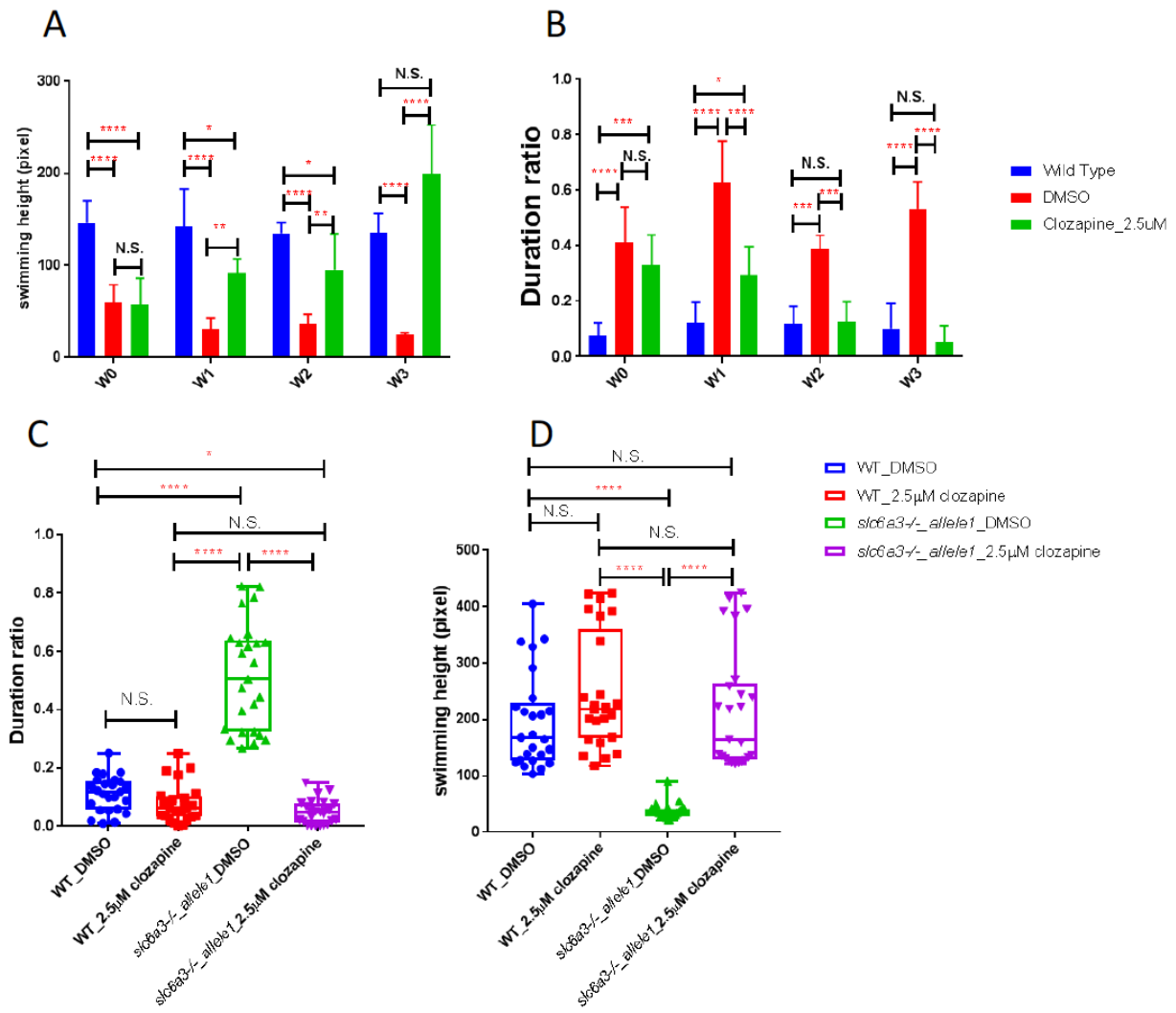

Supplementary Figure 4. Statistical analysis for 2.5uM clozapine treatment. (**A-B**), **related to Figure 3.** The bar-graphs of swimming height (**A**) and the "digging" behavior (**B)** from week zero (W0) to week 3 (W3) in WT, *slc6a3-/- allele1* treated by DMSO and 2.5uM clozapine in drug screen. n=5 for all. Error bar=standard deviation. *****p<0.0001; ***p<0.001; **p<0.01; *p<0.05,* N.S.= no significance. Significance test: one-way ANOVA Kruskal-Wallis test. (**C-D**) The box plots of swimming height (**C**) and the "digging" behavior (**D)** at week 3 in WT and *slc6a3-/- allele1* treated by DMSO and 2.5uM clozapine in a follow-up experiment. n=25 for all conditions. *****p<0.0001; ***p<0.001; *p<0.05,* N.S.= no significance. Significance test: one-way ANOVA Kruskal-Wallis test.

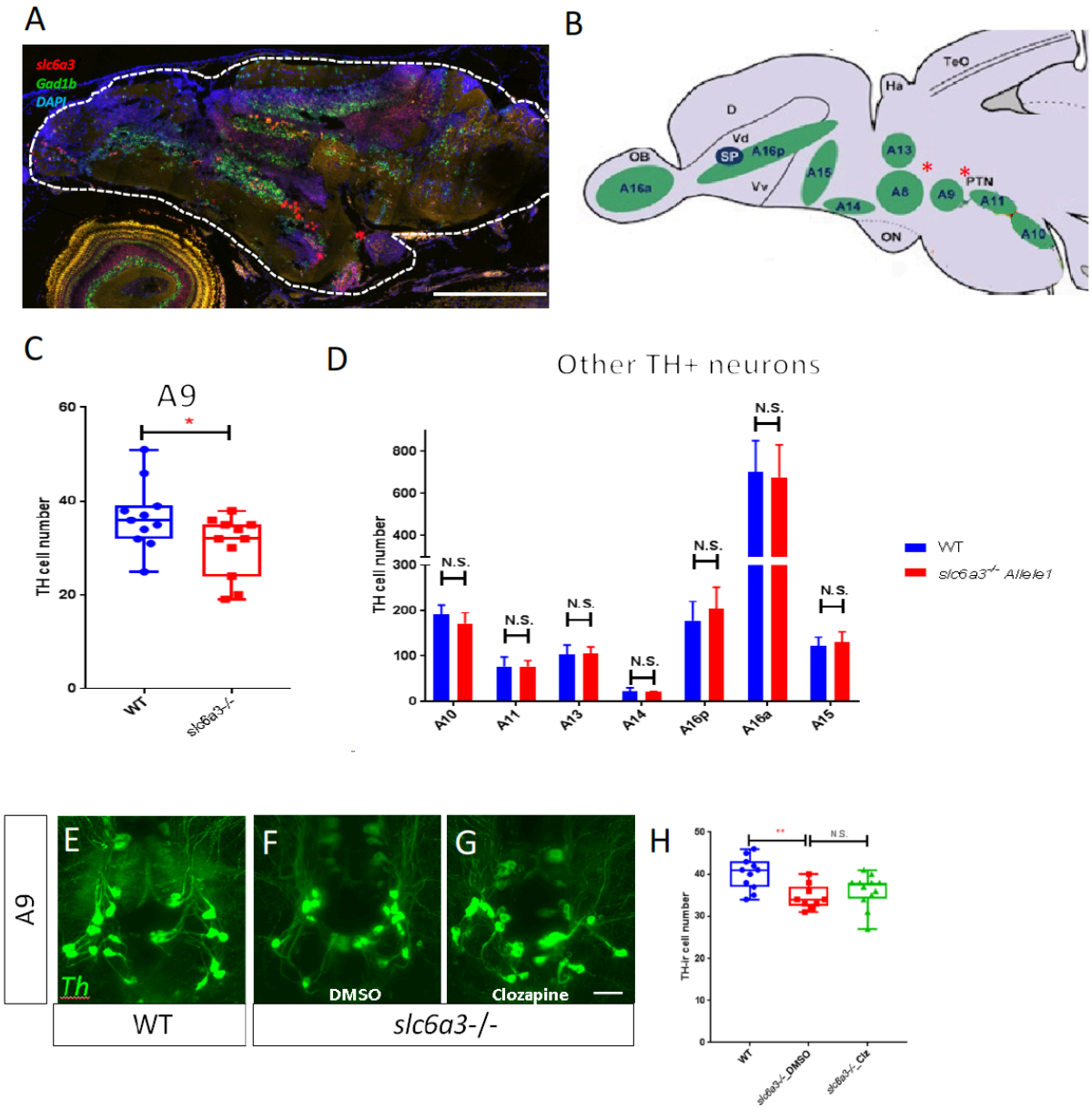

71

72 **Supplementary Figure 5. Whole brain CUBIC clearing to visualize TH+ neurons in the**
73 **adult brain, related to Figure 2 and Figure 3.** (**A**) RNAscope confirms expression of *slc6a3*
74 expression in the zebrafish brain. gad1b is a marker of brain glutamatergic neurons and used as
75 a reference of brain areas. Scale bar=250μm (**B**) Diagram of location of TH+ neuron groups
76 (dark green) in the zebrafish brain, in a sagittal view. D, dorsal telencephalic area; Ha,
77 habenula; OB, olfactory bulb; ON, optic nerve; PTN, posterior tuberculum; Vd, dorsal
78 telencephalic area; Vv, ventral telencephalic area; TeO, optic tectum; SP, Subpalium. **(Parker**
79 **et al., 2013) (C)** *slc6a3-/- allele1* fish manifest slight reduction of A9 DA neuron numbers at
80 2mpf. Box plot of cell numbers of A9 neurons are shown. Error bar=standard deviation. n=11 for

both WT and *slc6a3-/- allele1. *p<0.05.* Significance test: Wilcoxon–Mann–Whitney test. **(D)** TH+ neuronal number is unaffected in other regions of the *slc6a3-/- allele1* brain. Error bar=standard deviation. N>=8 for both WT and *slc6a3-/-* allele1 conditions. N.S.=no significance. Significance test: Wilcoxon–Mann–Whitney test. (**E-H**) 2.5uM clozapine treatment does not significantly rescue the A9 cell number in *slc6a3-/-* allele1. (**E-G**) Representative images of A9 neurons by z-projection of A9 neuron images. Scale bar=10μm. (**H**) Box plot of A9 DA cell number in wild-type, DMSO and 2.5uM clozapine treated *slc6a3-/- allele1* at 3mpf. For all n>=12. Error bar=standard deviation. **p<0.01.* N.S.=no significance. Significance test: one-way ANOVA Kruskal-Wallis test.

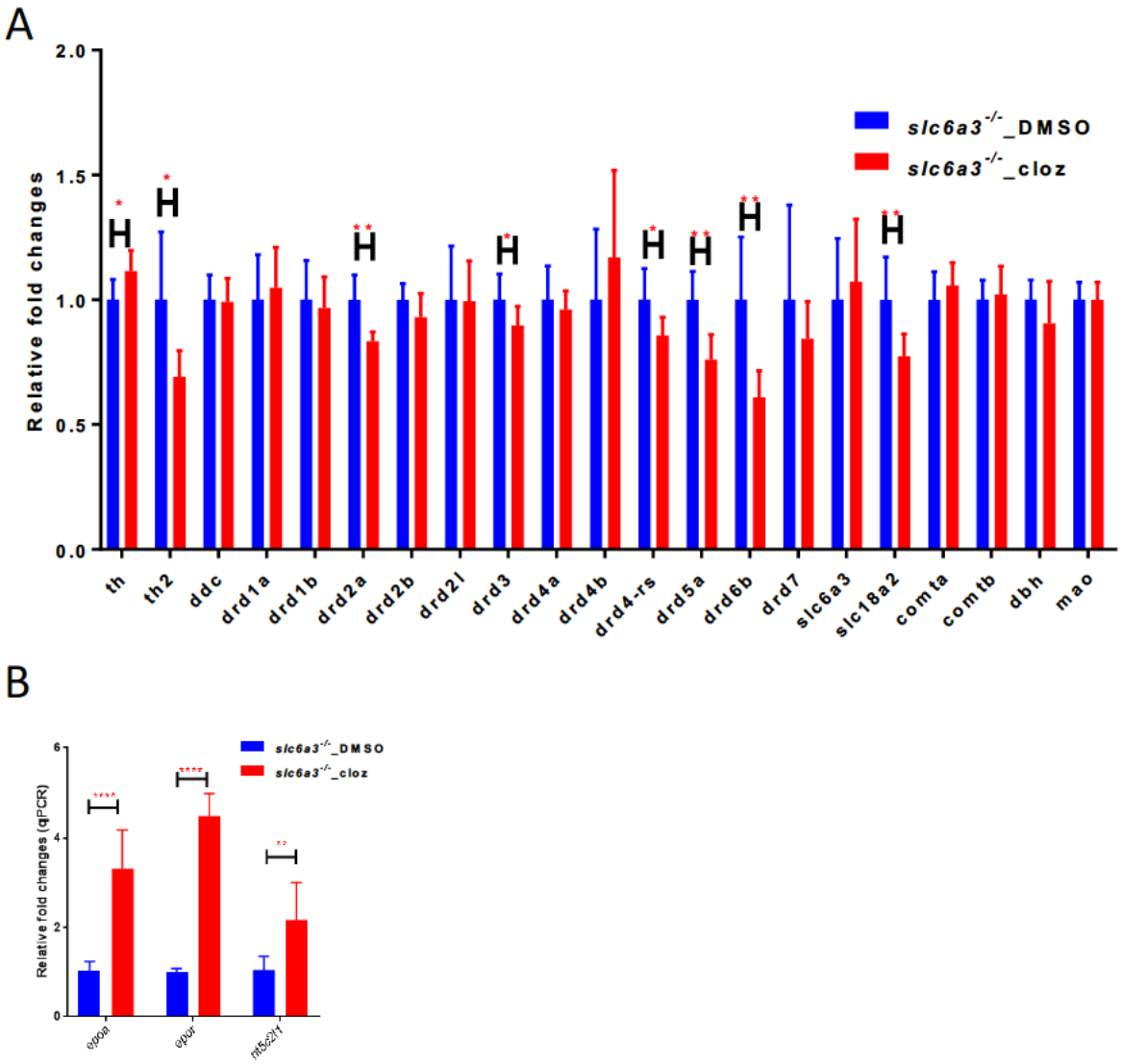

Supplementary Figure 6. Erythropoietin and 5'-nucleotidase pathway genes are upregulated by clozapine treatment in *slc6a3-/-* allele1, related to Figure 4. (**A**) The relative fold changes of all dopamine pathway genes by RNA-seq analysis, show minimal changes in gene expression levels. n=8 for all. Error bar=standard deviation. **p<0.05, *p<0.01.* N.S.=no significance. Significance test: Wilcoxon–Mann–Whitney test. (**B**) qRT-PCR confirms the up-regulations of *epoa, epor*, and *nt5c2l1* in slc6a3-/- allelel1 by 2.5uM clozapine treatment. n=6 for all. **p<0.01. ****p<0.0001.* Significance test: Wilcoxon–Mann–Whitney test.

Supplementary Video 1. Wild-type behavior, related to Figure 1.

Supplementary Video 2. *slc6a3-/-* allele1 behavior, related to Figure 1.

Supplementary Video 3. *slc6a3-/-* allele2 behavior, related to Figure 1.

Supplementary Video 4. *slc6a3-/-* allele1 behavior with 3-week DMSO treatment, related to Figure 3.

Supplementary Video 5. *slc6a3-/-* allele1 behavior with 3-week 2.5uM clozapine treatment, related to Figure 3.

Supplementary Video 6. *slc6a3-/-* allele1*;Tg(aTub:iTTA; TetO:EpoA-2a-GFP)* behavior at 2 months post fertilization, related to Figure 4.

Supplementary Excel table. Normalized RNA-seq counts of all genes in *slc6a3-/-* allele1 treated by DMSO and 2.5uM clozapine, related to Figure 4.

Transparent Methods

Animal husbandry

Zebrafish (*Danio rerio*) were housed in 3L tanks in a recirculating Aquatic Habitats facility (Pentair, USA) at 28±0.5°C water temperature. Fish were maintained on a 14-hour light/10-hour dark cycle with light turning on at 07:00 AM. Fish were fed a diet of brine shrimp (Catalog #BSEPCA-Brine Shrimp Direct, USA) twice daily and supplemented with flake fish food (Tetramin, Catalog# 98525-Pentair, USA) daily. All animals were maintained and procedures were performed in accordance with the Institutional Animal Care and Use Committees (IACUC) of NIBR.

Generation of the CRISPR mutants

The *slc6a3* CRISPR sgRNAs were designed based on an in-house genome assembly of the AB strain (unpublished, sequences available upon request). Two sgRNAs targeting different loci were selected (Table 1). sgRNAs were synthesized using T7 in vitro transcription using the MEGAshortscript™ T7 Transcription Kit (ThermoFisher, AM1354). Then sgRNAs were purified with MEGAclear™-96 Transcription Clean-Up Kit (ThermoFisher, 325 AM1909). The purified sgRNAs (125 ng/µL) were co-injected with Cas9 protein (500 ng/µL PNA bio, CP01) into 1-cell stage fertilized zebrafish embryos. CRISPR injected embryos were raised to adulthood and crossed with wild-type AB fish to get F1 generation. Mutants were identified in the F1 and maintained in heterozygous.

Behavioral assay

For behavioral analysis, we used a side-mounted camera (acA2000-165u mNIR, Basler) on a standard 1.4 L fish tank (Pentair, USA). To make the background uniform for tracking, a 25cmX25cm IR illuminating board was placed behind the fish tank for illumination. An optical filter (LP780-72 filter, MidOPT) was placed on a lens (LM8XC 1.3" (4/3") 8.5mm, F2.8, KOWA) to permit only infrared light being recorded. Five fish were netted into 1L fish water in the fish tank. After 5min acclimation, a 30min fish swimming video was recorded. The video dimension was 1224X500 (pixels). The recording frequency was 60hz. The video was tracked and annotated using Janelia Automatic Animal Behavior Annotator (JAABA) following the tutorial (http://jaaba.sourceforge.net) (Kabra et al., 2013). In total, eight 30min videos (240 minutes) were used for the "digging" classifier training (4 wild-type, 2 slc6a3-/- allele1, and 2 slc6a3-/- allele2). The parameters for training are: Iterations:100; Iterations for fast update: 10; Base Classifier: Decision Stumps; Sample points:2500; Bin:30; Cross Validation Fold: 7. All available features (appearance, social, locomotion, arena, position, identity, compatibility) were applied in the training. The weights of individual sub-features were ranked based on manual label (**Supplementary Figure 3B-E**). For the "digging" classifier, an accuracy of 94.1% was achieved in the positive frames (when fish show the "digging" behavior) and 98.2% in the negative frames (when fish do not show the "digging" behavior).

Whole brain immunofluorescence and TH+ cell counting

Whole brain immunofluorescence was adapted from the CUBIC clearing method (Susaki et al., 2015). Briefly, adult zebrafish were euthanized in ice-cold water and decapitated. The heads were fixed in 4% PFA for overnight at 4 °C. Then the brains were dissected and incubated in the Clearing reagent (250mg/mL urea; 250mg/mL N,N,N',N'-tetrakis (2-hydroxypropyl) ethylenediamine; 150mg/mL Triton X-100) at 37 °C with shaking for 4 days. The cleared brains were then incubated in blocking solution (1XPBS, 0.2% Triton X-100, 10% DMSO, 10% goat serum) at 37 °C for 1 day. The primary antibody (Anti-Tyrosine Hydroxylase (TH) , EMD Millipore, AB152) was added and incubated at 37 °C for 4 days. Following 1-day wash by wash solution (1XPBS, 0.1% Tween-20, 1% DMSO), the secondary antibodies (Alexa Fluor® 488 goat anti rabbit, ThermoFisher, A27034) were added an incubated at 37°C for 4 days. After 1 day wash, the samples were transferred into refractive index matching solution (RIMS) (30mL of 0.02 M phosphate buffer (Sigma P5244), 40g Histodenz (Sigma D2158), 0.1% Tween-20, 0.01% sodium azide, use NaOH adjust pH to 7.5) and imaged using a ZEISS lightsheet microscope with a 5X detection objective (Lightsheet Z.1, Zeiss). Images were processed using "lightsheet dualfusion" with default parameters in ZEN (Zeiss). Processed images were then

quantified using Arivis Vision4D software (Arivis Inc.) and FIJI (NIH). For counting of TH+ cells, the TH+ channel and the planes of interest were selected in ARIVIS Vision4D analysis panel. A filter of basic morphology (type: opening; radius:5) and a segmentation of blob finder (diameter 14um, threshold 17.32, high split sensitivity) were applied. After assessing the segmentation result we manually corrected the false positive segmentation. We used FIJI to generate all manuscript images.

RNA-seq and data process

Adult Zebrafish were euthanized by submersion in ice-cold water for 5min. The brains were dissected in RNAlater solution (ThermoFisher, AM7020). Total RNA from single zebrafish brains was prepared using the RNeasy Plus 96 Kit (Qiagen, 74192). mRNA libraries were generated using the TruSeq Stranded mRNA Library Prep Kit (Illumina, 20020595), and sequenced on Illumina HiSeq 2000 in paired-end mode. Four female and four male adult fish were sequenced for each condition at a mean depth of 34 million reads per sample. RNA sequencing reads were trimmed using Trimmomatic (version 0.32) to remove sequencing adaptors and low quality reads, mapped to internal zebrafish genome using STAR 2.5.3a with default parameters, and QCed using CollectRnaSeqMetrics from the picard-tools 1.113 package. An rRNA genome annotation generated using RepeatMasker prediction was downloaded from the UCSC genome browser and used for CollectRnaSeqMetrics; Uniquely mapped fragments were counted against a customized gtf file generated based on ENSEMBL zebrafish gene annotation (release 91). The featureCounts function (featureCounts -p -O -s 2) in the subread (version 1.5.0) package was used for counting. Differential brain gene expression analysis between DMSO and clozapine treatment was performed using DESeq2. The log2 fold changes were tested against 0 using the Wald test, and the p-values were adjusted using Benjamini-Hochberg multi-comparison correction.

Total RNA extraction and qRT-PCR

Adult Zebrafish were euthanized by submersion in ice-cold water for 5min. The brains were dissected in RNAlater solution (ThermoFisher, AM7020). Total RNA of zebrafish brain was prepared using RNeasy mini kit (Qiagen). The concentration of total RNA was measured and an equal amount of total RNA for all conditions was reverse transcribed using iScript™ Reverse Transcription Supermix (Bio-Rad, 1708840). The same amount of templates was used for qPCR with iTaq™ Universal SYBR® Green Supermix (Bio-Rad, 1725120) in QuantoStudio 7 Real-Time PCR (ThermoFisher Scientific). The sequences of all qPCR primers are listed in Table 2.

Cloning and overexpression of *epoa* in zebrafish brain

The *epoa* overexpression construct was cloned using a 3-way Gateway strategy based on the previously published Tol2kit cloning method (Kwan et al., 2007). A sequence of *epoa-2a-EGPF* flanked with a recombination sequence for the LR reaction were synthesized by Genewiz. A Gateway reaction was performed using LR Clonase™ II Plus enzyme (ThermoFisher, 12538120) to assemble three pieces of DNA fragments (5'-entry clone (TetO promoter), middle-entry clone (*epoa-2a-EGPF* cDNA), 3'- entry clone (PolyA tail)) into the destination vector (pDestTol2) at room temperature for overnight. The confirmed construct containing all DNA fragments (*TetO: epoa-2a-EGPF-PolyA*) was co-injected with a neuronal alpha-tubulin promoter driven itTA (*aTub:itTA*) and the Tol2 transposase mRNA in the *slc6a3*$^{-/-\_allele1}$ embryos at one-cell stage. The *epoa* expression level was verified by qRT-PCR of injected embryos at 5dpf. A stable transgenic line *slc6a3*$^{-/-\_allele1}$*; Tg(aTub:iTTA; TetO:EpoA-2a-GFP)* was screened by visualizing GFP fluorescence in the brain of progeny of injected fish.

Dopamine concentration measurement in whole zebrafish brains

Adult Zebrafish were euthanized using ice-cold water for 5min. The brains were dissected on an ice-cold stage and weighed using a Micro-balance (Mettler Toledo XPE56). The samples were randomized and transferred to Precellys tissue homogenizing CKmix tubes. Three hundred microliters of (70/30) acetonitrile/water containing 0.5% ascorbic acid and the dopamine internal standard 10 µM (Cambridge Isotopes d4) was added to each of the samples. The samples were homogenized at 2500 RPM for 3X30 seconds and then spun at 10,000 rpm for 10 minutes at 4°C. Fifteen microliters of the sample was transferred to a 384 well plate containing 30 µL of 100 mM borate buffer pH 9.0 and 15 µL of anhydrous acetonitrile containing 2% (v/v) benzoyl chloride (Sigma Aldrich) was added. The plate was sealed and shaken for 15 minutes. Calibration curves for dopamine starting at 125 µM were diluted 1:2 over 16 points. Calibration curves were treated the same as the samples. The samples and calibration curves were then transferred to an Agilent 1290 auto-sampler set a 4°C and 5 µL was injected onto a 2X50 mm ACE Excel 2 C18-Amide column connected to a Sciex 5500 operating in MRM mode. Solvent A was HPLC grade water containing 20 mM ammonium formate and 0.15% formic acid (v/v). Solvent B was HPLC grade acetonitrile. The flow rate was 600 µL per minute and the column was keep at a constant temperature of 60°C. The gradient was 100% A to 45% B over 5.5 minutes then to 51% B 4.5 minutes then a stepped to 95% B in 0.15 minutes and held at 95% B for 1 minutes. The column was then re-equilibrated at 0% percent A for 5 minutes. The mass

spectrometry parameters were Gas 1 30, Gas 2 20, CUR 30, Temp 450°C, collision gas 6, IonSpray Voltage 5500. The MRM for dopamine is 466.2-105.1 and for dopamine IS 470.2-105.1 DP 75, CE 40 and CXP 10. Dopamine eluted at 7.9 minutes. The data was processed using MutiQuant™. Dopamine concentrations were divided by the brain weights for normalization and then compared using JMP™ software by performing a t-test.

Supplementary Reference

Kabra, M., Robie, A.A., Rivera-Alba, M., Branson, S., and Branson, K. (2013). JAABA: interactive machine learning for automatic annotation of animal behavior. Nat Methods *10*, 64-67.

Kwan, K.M., Fujimoto, E., Grabher, C., Mangum, B.D., Hardy, M.E., Campbell, D.S., Parant, J.M., Yost, H.J., Kanki, J.P., and Chien, C.B. (2007). The Tol2kit: a multisite gateway-based construction kit for Tol2 transposon transgenesis constructs. Dev Dyn *236*, 3088-3099.

Parker, M.O., Brock, A.J., Walton, R.T., and Brennan, C.H. (2013). The role of zebrafish (Danio rerio) in dissecting the genetics and neural circuits of executive function. Front Neural Circuits *7*, 63.

Susaki, E.A., Tainaka, K., Perrin, D., Yukinaga, H., Kuno, A., and Ueda, H.R. (2015). Advanced CUBIC protocols for whole-brain and whole-body clearing and imaging. Nat Protoc *10*, 1709-1727.